13. Gordon, M. S.; Binkley, J. S.; Pople, J. A.; Pietro, W. J.; Hehre, W. J. *J. Am. Chem. Soc.* **1982**, *104*, 2797.
14. Pietro, W. J.; Francl, M. M.; Hehre, W. J.; Defrees, D. J.; Pople, J. A.; Binkley, J. S. *J. Am. Chem. Soc.* **1982**, *104*, 5039.
15. Gill, P. E.; Murray, W.; Wright, M. H. *Practical Optimization*; Academic Press, Inc.: New York, 1981.

Preparation and Characterization of Titanium Dioxide Embedded onto ZSM-5 Zeolite

A. Yu. Stakheev†, C. W. Lee, and P. J. Chong*

Advanced Materials Division, KRICT, P.O. Box 107, Yusung, Taejon 305-606, Korea
†N.D. Zelinsky Institute of Organic Chemistry, Leninskii Pr. 47, Moscow, Russia
Received October 19, 1997

Chemical vapor deposition of $TiCl_4$ followed by the hydrolysis thereof at elevated temperatures was employed for the formation of TiO_2 clusters inside ZSM-5 matrix. BET and XRD revealed that the zeolite structure remains intact. XPS, Raman, FTIR, and UV-VIS reflectance spectroscopy indicated that TiO_2 particles thus formed are extremely small and localized inside the zeolite matrix.

Introduction

Recently intensive research efforts have been directed toward the synthesis and characterization of "quantum-sized" semiconductor particles embedded inside zeolite framework.[1] Zeolites containing TiO_2 clusters may be of interest as a system for investigation into "quantum-size effect" (Q-size effect) and photoactive catalysts. Moreover, TiO_2-embedded zeolites may be useful for the preparation of shape-selective catalysts for the Fischer-Tropsch synthesis.[2]

Recently, two methods have been reported, whereby zeolite-hosted extra framework TiO_2 clusters are prepared.[3,4] These include ion exchange of Ti with ammonium titanyl oxalate aqueous solution, $(NH_4)_2TiO(C_2O_4)_2$, and chemical vapor deposition (CVD) of titanium by the treatment of zeolite with $TiCl_4$ vapors followed by the hydrolysis of the resulting material.

However, ZSM-5 zeolite containing TiO_2 clusters has not been prepared yet due to the difficulties in embedding of TiO_2 particles inside the narrow channel system of ZSM-5. The ion-exchange procedure does not allow the TiO_2 particles to be encapsulated inside the narrow pore zeolites (ZSM-5, mordenite, etc.), because TiO^{2+} are usually hydrated and too bulky to penetrate inside the zeolite pores. Treatment of the zeolite with $TiCl_4$ vapors appears to be more promising, but suffers from the damage of zeolite structure by HCl evolved due to the concurrent hydrolysis.

The main aims of this research are;

1) to develop the procedures for the encapsulation of ultra-fine nano-scale TiO_2 particles in ZSM-5 channels, which will not damage zeolite structure,

2) to study the effect of the TiO_2 inclusion on the zeolite structure, and

3) to characterize the resultant materials using relevant physico-chemical methods.

*To whom correspondence should be addressed.

Experimental

Sample preparation. ZSM-5 containing TiO_2 were prepared by chemical vapor deposition (CVD) of $TiCl_4$ onto HZSM-5 (Si/Al=15, PQ Co.). The order of preparative procedures are as follows:

1. Calcination
2. CVD of $TiCl_4$
3. Removal of excess $TiCl_4$
4. Hydrolysis of embedded $TiCl_4$

3-5 g of the zeolite powder was accurately weighed and loaded into a flow reactor with a diameter of 50 mm, which permits shallow bed spreads. It was calcined in O_2 flow overnight at 500 °C. Thereafter, dry helium was admitted with no further flow of oxygen. The experimental temperature was adjusted to 250-400 °C and CVD was performed for 3-4 hours. $TiCl_4$ vapor was diluted (1 : 10) with pure He so that the zeolite surfaces may not be damaged by the HCl evolved during the interaction of $TiCl_4$ with zeolite surface OH-groups. The overall flow rate of the mixed gas was about 300 mL/min. Treatment with $TiCl_4$ vapor was continued, until excess $TiCl_4$ was not observed in gas-wash bottle. Upon completion of the CVD step, the reactor was flushed for at least 2 hours at 500 °C to remove excess $TiCl_4$. Chemisorbed $TiCl_4$ was then hydrolyzed at 300-450 °C by a water vapor present in the flow of N_2. N_2 flow saturated with H_2O vapor was used after dilution (1 : 10) with pure N_2.

Sample characterization. The crystallinity of the samples was checked by X-ray diffraction (XRD) of the zeolite powder using a Rigaku D/MAX-3B diffractometer for which Cu-Kα radiation is employed. BET surface area was measured by physisorption of N_2 using a Micromeritics model, ASAP 2400. Raman spectra were measured by a

Jobin Yvon U-1000 spectrometer equipped with an Argon laser (25 mW at 514.5 nm) with a resolution of 0.15 cm^{-1}. The XPS measurement was carried out on an AEI ES-200B spectrometer within Al-target. The C_{1s} line (binding energy 285 eV) was used as an internal standard. Diffuse reflectance UV-VIS spectra of the zeolite powder were recorded on a Varian Cary 4 spectrophotometer equipped with an integrating sphere. Diffuse reflectance IR-spectra of OH-region were measured with a Nicolet 410 Impact equipped with a home-made diffuse-reflectacne attachment. Metal content was determined by atomic absorption spectroscopy (Perkin Elmer 2380 AAS). Microrpore volume was obtained from a t-plot method using a Micromeritics model, ASAP 2000.

Results and discussion

Effect of TiO_2 loaded onto zeolite structure. The characteristics of ZSM-5 before and after TiO_2 loading are summarized in Table 1 and Figure 1. The XRD pattern remains practically unaltered upon CVD followed by hydrolysis. The BET data also indicate that TiO_2 loading does not affect the zeolite surface profiles. Surface area and micropore volume remain unaltered within the limits of experimental error. These results show that the preparation procedure in use does not damage the zeolite structure due to TiO_2 deposition.

Table 1. BET data as observed from the deposition of TiO_2 onto zeolite pores

Sample	Surface area (m^2/g)	Micropore volume (cm^3/g)
HZSM-5, undeposited	428	0.196
TiO_2/ZSM-5, hydrolyzed at 300 °C	420	0.186
TiO_2/ZSM-5, hydrolyzed at 450 °C	421	0.189

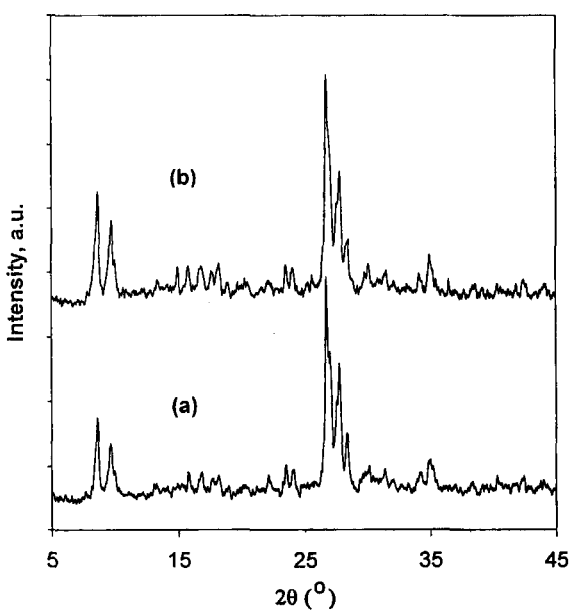

Figure 1. Powder X-ray diffraction patterns of (a) initial HZSM-5, and (b) TiO_2/ZSM-5 hydrolyzed at 400 °C.

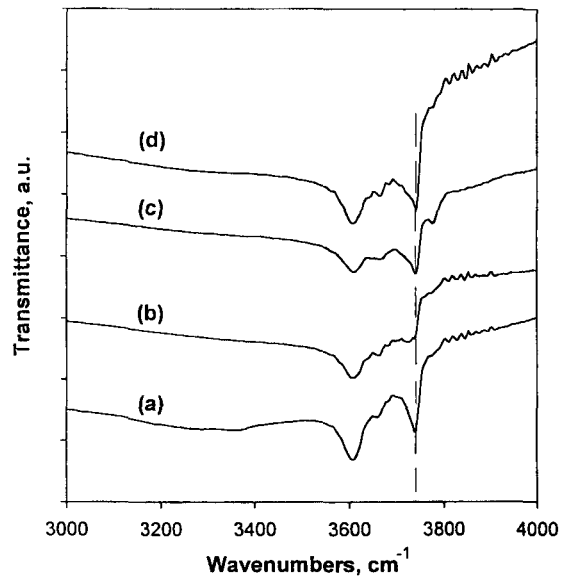

Figure 2. FT-IR spectra showing the variation of OH bands intensity at 3740 and 3610 cm^{-1} with Ti-deposition. (a) initial HZSM-5. (b) after $TiCl_4$ CVD. (c) with hydrolysis at 300 °C, and (d) with hydrolysis at 450 °C.

FTIR spectra of the OH group region (Figure 2) show that $TiCl_4$ deposition results in the significant decrease in the OH-band intensity at 3740 cm^{-1} which corresponds to terminal -Si-OH groups. The subsequent hydrolysis restores the band intensity.[5] On the other hand the band at 3610 cm^{-1} still decreases in intensity after $TiCl_4$ treatment and restores in intensity after hydrolysis at 450 °C, though these changes are not so pronounced as for the band at 3740 cm^{-1}. Probably this is due to the fact that terminal hydroxyls are easier for access by bulky $TiCl_4$ molecules than bridged hydroxyls. This is in a good agreement with the viewpoint that during CVD the reaction of $TiCl_4$ with zeolite (Z) OH groups will occur as follows:

$$\text{Z-OH} + TiCl_4 \Rightarrow \text{Z-O-}TiCl_3 + HCl \quad (1)$$

The subsequent hydrolysis cleaves the Z-O-Ti bond, restoring the zeolite (Z) OH groups:

$$\text{Z-O-}TiCl_3 + 4H_2O \Rightarrow \text{Z-OH} + Ti(OH)_4 + 3HCl \quad (2)$$

Location of Ti species. The data on Ti/Si atomic ratios as obtained from AAS (bulk analysis) and XPS (surface composition) are presented in Table 2. The AAS results are almost the same as those of XPS within experimental error. This indicates that Ti species are uniformly distributed inside zeolite matrix without localization onto the zeolite external surface.

Formation and structure of Ti species. The formation of TiO_2 species in zeolites is illustrated by the XPS data (Figure 3). As Figure 3 demonstrates, two types of Ti-species are revealed from Ti-containing zeolites. The peak at lower binding energy (~458 eV) is the TiO_2 particles characteristic of octahedral coordination. The peak at higher binding energy (~460 eV) may be attributed to the Ti ions of lower coordination, tetra-, or pentahedral, presumably due to those in cationic positions ($Ti_{cat.}$).[6]

Table 2. Compositional change of Ti/Si with respect to surface and bulk of TiO_2-containing ZSM-5 samples

ZSM-5 modification \ Method	Elemental analysis for Ti/Si molar ratio	
	Bulk via AAS	Surface *via* XPS
CVD of $TiCl_4$ at 300 °C	0.035	0.037
CVD at 300 °C, hydrolyzed at 300 °C	0.033	0.035
CVD at 300 °C, hydrolyzed at 450 °C	0.041	0.038

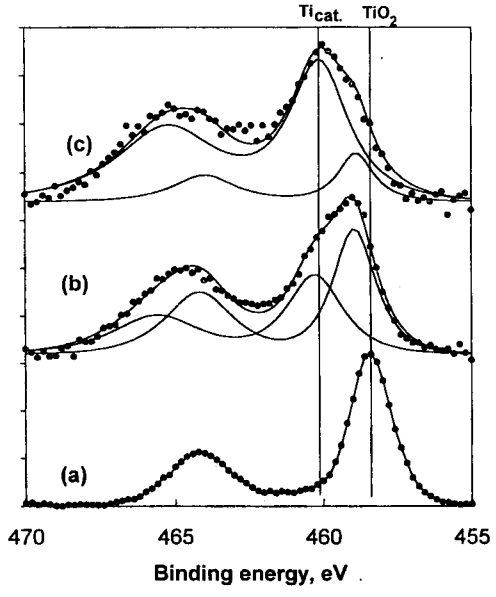

Figure 3. Variation of Ti 2p XPS spectra with (a) TiO_2. (b) TiO_2/ZSM-5 hydrolyzed at 450 °C. and (c) TiO_2/ZSM-5 hydrolyzed at 300 °C.

As shown in Figure 3, the hydrolysis at lower temperatures, say at 300 °C, transforms only a minor part of Ti ions into TiO_2 particles (−458 eV). However, with increase in hydrolytic temperatures up to 450 °C, this peak is predominant in the spectra. This indicates that the TiO_2 particles are formed more intensively at elevated temperatures.

This conclusion is in agreement with the data of Raman spectroscopy. Figure 4 shows the Raman spectra of Ti containing zeolites after the CVD of $TiCl_4$ followed by the hydrolysis at different temperatures. As Figure 4 indicates, the hydrolysis at 300 °C gives the intensity of the Raman vibration at 144 cm^{-1}, being characteristic of TiO_2-phase, which is rather low. However, the increase in hydrolytic temperatures leads to the marked increase in the band intensity.

Evidence indicates that hydrolytic temperature is an important factor, governing the structure of Ti-species. After the hydrolysis at lower temperatures, most of Ti ions remain within the cationic positions, which are occupied by the CVD of $TiCl_4$ according to the reaction (1). Higher temperatures are required for hydrolysis, and at 400-450 °C the majority of Ti ions is found to be converted into TiO_2 particles.

The diffuse reflectance UV-VIS spectra for the Ti-containing zeolites and for bulk titania are shown in Figure 5. A significant blue shift is observed for the Ti-containing zeolites, as compared to that of bulk TiO_2. For TiO_2 the onset is *ca.* 425 nm. For Ti/ZSM-5 two types of Ti-species can be distinguished-with the onset of *ca.* 325 and 380 nm, respectively. The significant blue shift indicates that the TiO_2 particles are extremely small.[3,4] This phenomena may occur when the particle size becomes small enough to be comparable to the de Broglie wavelength of a charge carrier. The effective mass of an electron in a crystal lattice often is substantially smaller than that of an elecron in free space; *i.e.*, the de Broglie wavelength is rather long and therefore the effects can be seen in particles a few nanometers in diameter. The size quantization effects occur most drastically in low band gap materials where the effective mass of the electron is particularly small.[7(b)] The XPS data confirm this conclusion. The peak of TiO_2 phase in XPS spectra (~458 eV) is shifted to higher binding energy by 0.8-1.0 eV re-

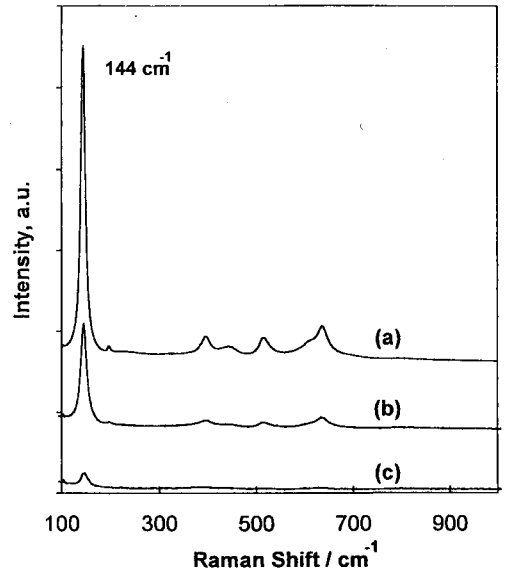

Figure 4. Raman spectra of (a) TiO_2. (b) TiO_2/ZSM-5 hydrolyzed at 450 °C, and (c) TiO_2/ZSM-5 hydrolyzed at 300 °C.

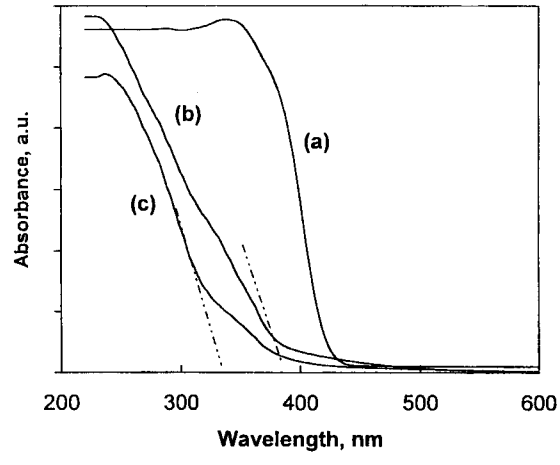

Figure 5. Diffuse reflectance UV-VIS spectra of (a) TiO_2. (b) TiO_2/ZSM-5 hydrolyzed at 450 °C. and (c) TiO_2/ZSM-5 hydrolyzed at 300 °C.

lative to that of the bulk TiO_2. This shift indicates that the TiO_2 particles inside ZSM-5 framework are extremely small and size-dependent.

It was interested to note that two types of TiO_2 species are present, as demonstrated by UV-VIS spectroscopy. This phenomena may tentatively be explained as follows. The onset of *ca.* 325 nm might be attributed to the formation of nanoscale TiO_2 clusters inside the zeolite cavities formed by channel intersections. The second type of the TiO_2 particles may be involved with the onset of *ca.* 380 nm, which might be rod-like particles grown inside the zeolite channels. The formation of analogous particles has been reported earlier for the zeolites with different channel structure, *viz* mordenite and L zeolite.[4]

Conclusions

1. The procedure developed for the TiO_2 deposition on ZSM-5 zeolite does not cause any marked damage of the zeolite structure.

2. The TiO_2 paticles embedded are uniformly distributed inside the zeolite framework without localization onto the zeolite external surfaces.

3. The TiO_2 particles thus embedded appear to be small enough to exhibit the properties typical of quantum-sized particles.

References

1. (a) Stucky, G. D.; Mac Dougall, J. E. *Science* **1990**, *247*, 669. (b) Ozin, G. A. *Adv. Mater.* **1992**, *4*, 612. *Stud. in Surf. Sci. & Catal.* **1997**, *105*, 1077.
2. Komaya, T.; Bell, A. T.; Weng-Sieh, Z.; Gronsky, R.; Engelke, F.; King, T. S.; Pruski, M. *J. Catal.* **1994**, *150*, 400.
3. Klaas, J.; Kulawik, K.; Schulz-Ekloff, G.; Jaeger, N. I. *Stud. Surf. Sci. Catal.* **1994**, *84*, 2261.
4. Liu, X.; Iu, K.-K.; Thomas, J. K. *J. Chem. Soc., Faraday Trans.* **1993**, *89*, 1861.
5. Haukka, S.; Lakomaa, E.-L.; Root, A. *J. Phys. Chem.* **1993**, *97*, 5085.
6. Blasco, T.; Camblor, M. A.; Perez-Pariente, J. *J. Am. Chem. Soc.* **1993**, *115*, 11806.
7. (a) Brus, L. E. *J. Chem. Phys.* **1983**, *79*, 5566. (b) Henglein, A. *Chem. Rev.* **1989**, *89*, 1861.

Microstructure, Electrical Property and Nonstoichiometry of Light Enhanced Plating (LEP) Ferrite Film

Don Kim*, Choong Sub Lee†, and Yeong Il Kim

Department of Chemistry, †Department of Physics,
Pukyong National University, Pusan 608-737, Korea
Received November 15, 1997

A magnetic film was deposited on a slide glass substrate from aqueous solutions of $FeCl_2$ and $NaNO_2$ at 363 K. XRD analysis showed that the film was polycrystalline magnetite ($Fe_{3(1-\delta)}O_4$) without impurity phase. The lattice constant was 0.8390 nm. Mössbauer spectrum of the film could be deconvoluted by the following parameters: isomer shifts for tetrahedral (T_d) and octahedral (O_h) sites are 0.28 and 0.68 mm/s, respectively, and corresponding magnetic hyperfine fields are 490 and 458 kOe, respectively. The estimated chemical formula of the film by the peak intensity of Mössbauer spectrum was $Fe_{2.95}O_4$. Low temperature transition of the magnetite (Verwey transition) was not detected in resistivity measurement of the film. Properties of the film were discussed with those of pressed pellet and single crystal of synthetic magnetites. On the surface of the film, magnetite particles of about 0.2 μm in diameter were identified by noncontact atomic force microscopy (NAFM) and magnetic force microscopy (MFM).

Introduction

Thin liquid film plating technique invented by Abe *et al.*[1] is a very useful method to synthesize magnetite thin films from aqueous solution at low temperature, especially below 100 °C.[1] They found that light irradiation during the plating process (Light Enhanced Plating: LEP) increases the film deposition rate due to the local heating effect.[2] LEP technique has many advantages: high deposition rate (~0.3 μm/min),[2,3] easy doping of foreign atoms ($Fe_{3-x}M_xO_4$; M=transition metal),[3] and mass production of films.[1] And various materials (glass, quartz, semiconductors and most of polymers) could be used as a substrate for LEP technique.[3] The ferrite films prepared by this method are strongly compatible with water and some organic compounds due to hydrophilic nature of ferrite film structure.[4] Therefore, the ferrite films have many potential applications from bio-sensors to electronic devices.[5-7]

Many works have been reported for the surface of magnetites since scanning probe microscope (SPM) was invented.[8] For example, Wiesendanger *et al.* reported[9] ord-